Phase Transitions

DOI: 10.1002/anie.201308039

Melting at High Pressure: Can First-Principles Computational Chemistry Challenge Diamond-Anvil Cell Experiments?**

Jonas Wiebke, Elke Pahl,* and Peter Schwerdtfeger**

Dedicated to Professor Helmut Schwarz on the occasion of his 70th birthday

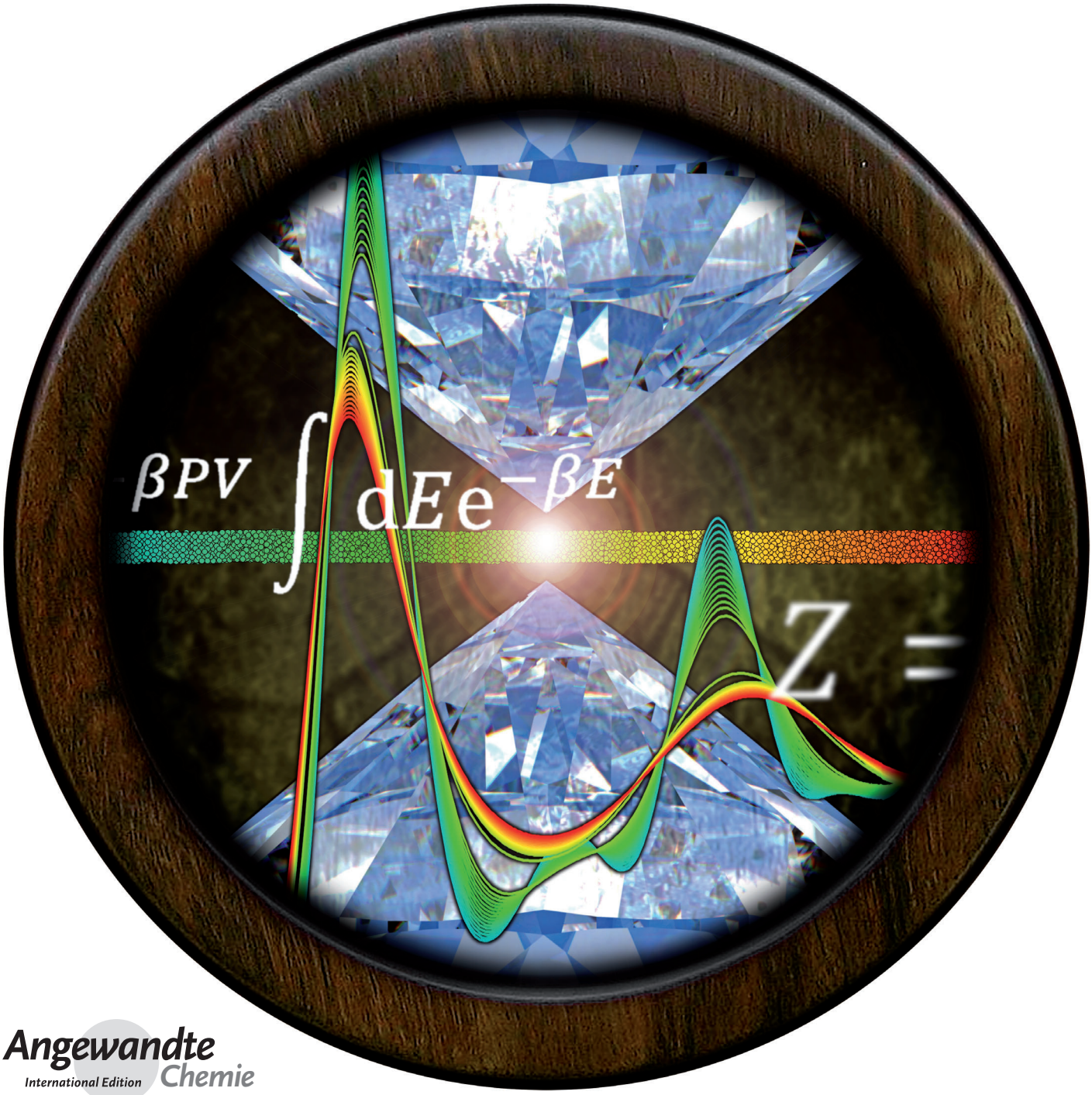

© 2013 Wiley-VCH Verlag GmbH & Co. KGaA, Weinheim

Understanding the phase behavior and properties of matter at high-pressure conditions is of fundamental importance for a great variety of applications[1] ranging from material science[2] to the chemistry and physics of the interior of planets and stars.[3,4] In Earth's inner core boundary, for example, pressures well exceed 300 GPa (about 3×10^6 atmospheres).[3] At these conditions, core and lower mantle properties (for example, the melting temperature of iron, a quantity decisive for our planet's interior structure and dynamics) have to be inferred by extrapolation from diamond-anvil cell (DAC) experiments.[3,5] While the great difficulties of this approach are very well exemplified by substantial discrepancies in the melting curve of iron above 100 GPa,[5] the situation is similar even for most simple substances such as argon. Freezing to a face-centered cubic crystal at 83.8 K and ambient pressure, the melting curve of Ar has been established to follow a Simon law up to a few gigapascals.[6–11] Beyond, however, lies a regime where data sets and extrapolants diverge.[12]

Modern computational chemistry enables a strategy different from extrapolation. Given a model of intermolecular forces accurate and consistent over the relevant range of compression, high-pressure phases can be simulated directly. Herein we report the melting curve of argon predicted from ab initio Monte Carlo simulations of the fcc crystal and liquid phases. Employing accurate analytic many-body potentials derived from rigorous relativistic electronic structure calculations, we observe corresponding-state behavior, that is, a Simon law, up to 100 GPa in quantitative agreement with a 2008 meta-analysis.[9] As shown in Figure 1, our simulations exceed the highest pressure experimentally achieved for melting argon.

Modern DACs routinely achieve pressures in the gigapascal range, but accurate observation of high-pressure melting remains extremely challenging. Broadly speaking, problems can be classified in two categories: arising from the difficulties to unambiguously identify melting of the sample, and from the intricacies of temperature (and pressure) measurement. First, although structural changes in samples are readily observed, laser speckle methods[3,8,11] cannot reveal the nature of such changes. X-ray diffraction patterns[5a] probe for a periodic bulk structure only. Premelting phenomena, which are amplified by shear stress in the DAC[13a,b] and use of pressure media,[13b,c] further complicate the situation. Second, temperature is usually measured by fitting the sample spectral irradiance to a Planck law,[3,11] often

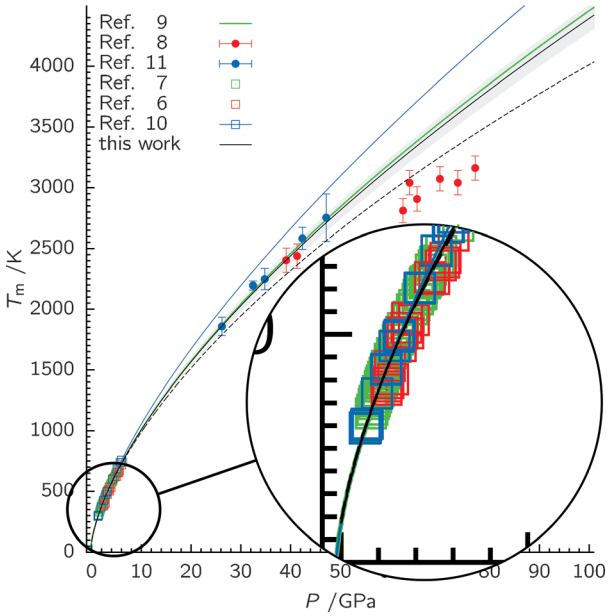

Figure 1. Melting temperature $T_m(P)$ of argon as a function of pressure P up to 100 GPa. The ab initio melting curve reported herein is drawn as solid black line; a gray band represents the estimated uncertainty of ±2.6%. The dashed black line is the melting curve obtained from the pairwise-additive approximation (omitting many-body effects).

involving ad-hoc simplifications regarding the variability of sample emissivity with wavelength, temperature, pressure, and surface quality. Inaccuracies in temperature can easily propagate to errors in pressure if optical pressure sensors are used.[14] Last but not least, high-pressure challenges chemical intuition.[15] Not only may samples form carbides with the actual diamond anvil at high temperatures and pressures;[5b,13c] near 25 GPa, tantalum, for example, even reacts with argon![13c] Given these factors, the difficulties in measuring high-pressure melting curves can hardly be understated.

Simulations of the melting transition face a different set of problems. Thermodynamic integration requires anchors to somewhat artificial reference states and stable, reversible connecting paths.[16] Molecular dynamics (MD) simulations of periodic systems suffer from large hysteresis effects and superheat to temperatures $T > T_m$ in the absence of free surfaces.[17] A class of "void methods" nucleates melt at lattice defects to avoid superheating,[18] but generating the defective initial configurations is generally unsystematic. Lastly, the solid–liquid interface can be modeled explicitly,[18c] but this approach is computationally very demanding.

Herein we choose a different approach and infer the melting temperature T_m by considering the superheated solid state. Within a parallel-tempering Monte Carlo framework,[19] we perform constant-pressure simulations of a supercell of 256 Ar atoms for a range of temperatures from below T_m to beyond the solid–liquid transition temperature. As we employ periodic boundary conditions, the solid superheats to temperatures $T > T_m$ before structural collapse occurs at the "critical superheating temperature" T^+ well above T_m. We observe this transition as a distinct, sharp maximum in the heat capacity C_P as shown in Figure 2. Judged by the pair distribution function $g(r;P,T)$, this maximum coincides with the breakdown of long-

[*] Dr. J. Wiebke, Dr. E. Pahl, Prof. Dr. P. Schwerdtfeger
Centre for Theoretical Chemistry and Physics (CTCP)
The New Zealand Institute for Advanced Study, NZIAS, and
The Institute of Natural and Mathematical Sciences, INS
Massey University Albany
Private Bag 102904, Auckland 0745 (New Zealand)
E-mail: j.wiebke@massey.ac.nz
e.pahl@massey.ac.nz
p.a.schwerdtfeger@massey.ac.nz

[**] J. Wiebke is indebted to the Deutscher Akademischer Austauschdienst (DAAD) for funding and support during the first two-year period of his stay in Auckland. We thank Dr. Florian Senn for useful discussions.

 © 2013 Wiley-VCH Verlag GmbH & Co. KGaA, Weinheim

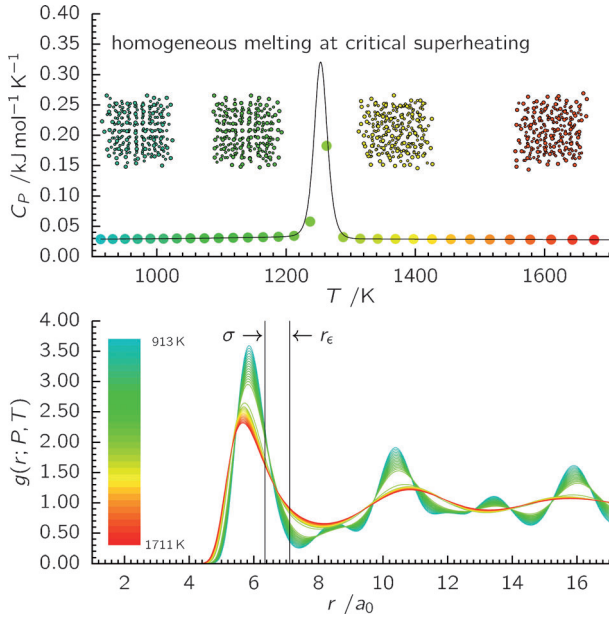

Figure 2. Top: Temperature dependence of the molar isobaric heat capacity C_P of argon at 10 GPa. Also shown are snapshots of configurations of the Ar_{256} supercell below and above homogeneous melting at critical superheating at $T^+ = 1254$ K. Bottom: Corresponding pair distribution function $g(r;P,T)$ between 913 and 1711 K. Near T^+, the fcc lattice breaks down to form a disordered fluid. The van-der-Waals radius σ and well minimum distance r_ϵ of the pair potential are indicated.

range order and can thus be interpreted as latent heat of homogeneous, that is, defect-free melting. Superheating and homogeneous melting has been observed in shock heating experiments[17a,20] and MD simulations.[17a,c,18a] Moreover, a microcanonical analysis[17c] suggests to relate the temperatures of melting and the solid–liquid transition at critical superheating via Equation (1):

$$\lim_{P\to\infty} T^+/T_m = 1 + \ln 2^{1/3} \qquad (1)$$

Herein we use this connection to obtain the melting temperature $T_m \approx T^+/1.231$ directly from the critical superheating temperature T^+. Although approximate in nature,[17c] Equation (1) turns out to be of remarkable accuracy across a wide range of pressures.

From simulations up to pressures of 100 GPa, we obtain a smooth Kechin form:[21]

$$T_m(P) = (80.4\ \mathrm{K})(P/0.201\ \mathrm{GPa} + 1)^{1/1.552} \exp(-0.634\ \mathrm{kPa}^{-1}\ P) \qquad (2)$$

with an estimated uncertainty of $\pm 2.6\,\%$ in T_m. At standard atmospheric pressure, Equation (1) is expected to be least-accurate. Yet we compute a bulk melting temperature of 80.4 ± 2.1 K, which is only slightly smaller than the NIST-recommended value[22] of 83.3 ± 0.3 K. Similar simulations of finite Ar_N clusters provided an estimate of 86.3–87.0 K.[23] With rising pressure, our ab initio melting curve is in excellent agreement with the measurements of Datchi et al.[7] A bias of the most recent DAC experiments[10] towards higher melting temperatures becomes apparent at elevated pressures. At and above 40 GPa, our ab initio melting curve agrees with the high-pressure data set of Jephcoat and Besedin,[11] but is at variance with the observations of Boehler et al.[8] The small Kechin exponent of only 0.634×10^{-6} GPa^{-1} effectively renders our ab initio melting curve a Simon law on the gigapascal scale. In fact, the deviations from corresponding-state behavior as observed by Boehler et al.[8] have been suggested to be an experimental artefact.[12]

As shown in Figure 1, our ab initio melting curve agrees with the smooth fit of Ferreira's and Lobo's meta-analysis[9] over the entire pressure and temperature range. For example, at 100 GPa, we compute T_m to 4409 ± 132 K; Ferreira and Lobo extrapolate to 4357 to 4451 K.[9] It cannot be overstated that here we do not achieve this level of agreement from extrapolation of sufficiently accurate low-pressure data, but from interpolation of high-pressure melting temperatures simulated directly.

The interaction of noble gas atoms is usually described by a Lennard-Jones potential, $\Phi_{LJ}(r) = 4\varepsilon[(\sigma/r)^{12} - (\sigma/r)^6]$, with well depth ε and van-der-Waals radius σ. In contrast, we attribute the success of our approach to the accuracy of the ab initio many-body potentials employed,[24,25] obtained from highly accurate potential surfaces through relativistic wave-function-based electronic structure calculations. No empirical parameters enter these calculations. Simulation of high-pressure melting illustrates both the requirements on the interaction model as well as the predictive power of such an ab initio approach. Clearly, as seen in Figure 1 for the melting curve obtained by omitting the many-body potentials, many-body effects are crucial for a quantitative picture even at relatively moderate pressures. The importance of an accurate repulsive branch $r < \sigma$ of the pair potential is even greater and can be illustrated as follows: at 100 GPa and 4000 K, we find a mean fcc lattice constant of $7.037\,a_0$ as compared to the (zero-temperature) minimum-energy value of $10.024\,a_0$. This corresponds to an almost three-fold compression in volume. Integration over the pair distribution function $g(r;P,T)$ up to the van-der-Waals radius of the pair potential, $\sigma = 6.345\,a_0$, yields an average of more than 12 atoms within the repulsive domain. Consequently, "squeezing out van-der-Waals space" does require particular attention to the short-range, strongly repelling interaction components.[15] Using a Lennard-Jones potential with its only qualitatively correct, repulsive $1/r^{12}$ term, we obtain a 100 GPa melting temperature of well over 7000 K.

Given the excellent agreement with a number of experimental data sets for low to moderate pressures as well as the first-principle, parameter-free nature of our interaction model, we believe that our ab initio melting curve of argon is quantitatively correct up to 100 GPa. We expect our simulation procedure to be further refined by inferring the melting temperature more rigorously and accurately than via Equation (1),[26] particularly near standard atmospheric pressures, and by melting from hexagonal close-packed[27] and body-centered cubic phases.[12a,b] However, we do not expect the hcp and bcc melting curves to be appreciably different.[12a] Yet we feel that a definite prediction of solid–liquid coexistence must not be in ignorance of the solid phase behavior across the pressure range of interest. The high-pressure phase

 © 2013 Wiley-VCH Verlag GmbH & Co. KGaA, Weinheim

diagram of argon (especially the precise location of a fcc–hcp–liquid or fcc–bcc–liquid triple point, if it exists)[9,12a,b] remains highly controversial.

In conclusion, having demonstrated that first-principle computational chemistry can indeed challenge diamond-anvil experiments of high-pressure melting, we acknowledge that the case of argon is arguably the most simple. The lighter noble gases, neon and helium, are difficult to near impossible to be described by classical dynamics; the better part of the remaining Periodic Table is made from electron-deficient elements, forming strongly interacting semiconducting or metallic bulk phases with rich phase diagrams. Although some progress has been made, for the noble gases[23a,28] as well as for mercury,[29] the real challenges for computational chemistry still lie ahead.

Methods

We employ a parallel-tempering Monte Carlo scheme[19] to sample from isobaric–isothermal ensembles with periodic boundary conditions,[16] effectively allowing the supercell volume to fluctuate at constant pressure and temperature. Typical production simulations propagate 32 trajectories of Ar_{256} at temperatures geometrically distributed over an interval including T_m and T^+. We use a many-body decomposition of the total interaction energy truncated after the three-body contributions Φ_3, applying the minimum image convention and a spherical cut-off of $12.5\,a_0$, less than half the supercell length at the largest compression achieved. We employ Patkowski's and Szalewicz's pair potential[24] with standard long-range corrections[16] and our ab initio three-body potential[25] for Φ_3. The extended Axilrod–Teller–Muto form of Φ_3 has been shown to perform excellently for solid neon up to high pressures and temperatures.[30] We obtained smooth $C_P(T)$ curves by accumulating histograms of the isobaric–isothermal Boltzmann distributions and subsequent reweighting;[31] T^+ is taken as maximizer of C_P. Equation (2) has been obtained from fitting to simulations at 1 bar and 1, 5, 10, 50, and 100 GPa. Our error estimate of $\pm 2.6\%$ in T_m is a two-standard deviation over four statistically independent simulations. Within this accuracy, our simulation procedure is robust with respect to the number of equilibration and sampling cycles, interaction cut-off, and supercell size.

Received: September 12, 2013
Published online: November 7, 2013

Keywords: argon · high pressure · melting · Monte Carlo simulations · superheating

[1] *Industrial High Pressure Applications* (Ed.: R. Eggers), Wiley-VCH, New York, **2012**.
[2] a) P. F. McMillan, *Nat. Mater.* **2002**, *1*, 19 – 25; b) J. S. Schilling, J. J. Hamlin, *J. Phys. Conf. Ser.* **2008**, *5*, 052006.
[3] R. Boehler, *Rev. Geophys.* **2000**, *38*, 221 – 245.
[4] T. S. Duffy, *Nature* **2008**, *451*, 269 – 270.
[5] a) S. Anzellini, A. Dewaele, M. Mezouar, P. Loubeyre, G. Morard, *Science* **2013**, *340*, 464 – 466; b) S. Tateno, K. Hirose, Y. Ohishi, Y. Tatsumi, *Science* **2010**, *330*, 359 – 361.
[6] C. S. Zha, R. Boehler, D. A. Young, M. Ross, *J. Chem. Phys.* **1986**, *85*, 1034 – 1036.
[7] F. Datchi, P. Loubeyre, R. LeToullec, *Phys. Rev. B* **2000**, *61*, 6535 – 6546.
[8] R. Boehler, M. Ross, P. Söderlind, D. B. Boercker, *Phys. Rev. Lett.* **2001**, *86*, 5731 – 5734.
[9] A. G. M. Ferreira, L. Q. Lobo, *J. Chem. Thermodyn.* **2008**, *40*, 618 – 624.
[10] E. H. Abramson, *High Pressure Res.* **2011**, *31*, 549 – 554.
[11] Curiously, at about 47 GPa both Fe and Ar melt at the same temperature of 2750 ± 200 K; see A. P. Jephcoat, S. P. Besedin, *Philos. Trans. R. Soc. London Ser. A* **1996**, *354*, 1333 – 1360.
[12] a) F. Saija, S. Prestipino, *Phys. Rev. B* **2005**, *72*, 024113; b) A. B. Belonoshko, S. Davis, A. Rosengren, R. Ahuja, B. Johansson, S. I. Simak, L. Burakovsky, D. L. Preston, *Phys. Rev. B* **2006**, *74*, 054114; c) E. Pechenik, I. Kelson, G. Makov, *Phys. Rev. B* **2008**, *78*, 134109.
[13] a) U. Tartaglino, T. Zykova-Timan, F. E. Ercolessi, E. Tosatti, *Phys. Rep.* **2005**, *411*, 291 – 321; b) S. V. Starikov, V. V. Stegailov, *Phys. Rev. B* **2009**, *80*, 220104; c) A. Dewaele, M. Mezouar, N. Guignot, P. Loubeyre, *Phys. Rev. Lett.* **2010**, *104*, 255701.
[14] The widely used ruby gauge exploits luminescence from the split ^2E_g levels to the high-spin $^4A_{2g}$ ground state of $(3d^3)$ Cr^{3+} dopants in the corundum lattice. Width and spectral position of the resulting R_1 line depend on pressure and temperature, but the interdependence of these effects remains to be understood. For details, see: a) A. F. Goncharov, J. M. Zaug, J. C. Crowhurst, E. Gregoryanz, *J. Appl. Phys.* **2005**, *97*, 094917; b) K. Syassen, *High Pressure Res.* **2008**, *28*, 75 – 126.
[15] W. Grochala, R. Hoffmann, J. Feng, N. W. Ashcroft, *Angew. Chem.* **2007**, *119*, 3694 – 3717; *Angew. Chem. Int. Ed.* **2007**, *46*, 3620 – 3642.
[16] D. Frenkel, B. Smit, *Understanding Molecular Simulation*, Academic Press, San Diego, **2002**.
[17] a) S. N. Luo, T. J. Ahrens, T. Cagin, A. Strachan, W. A. Goddard III, D. C. Swift, *Phys. Rev. B* **2003**, *68*, 134206; b) L. Gómez, C. Gazza, H. Dacharry, L. P. Penaranda, A. Dobry, *Phys. Rev. B* **2005**, *71*, 134106; c) A. B. Belonoshko, N. V. Skorodumova, A. Rosengren, B. Johansson, *Phys. Rev. B* **2006**, *73*, 012201.
[18] a) J. Solca, A. J. Dyson, G. Steinebrunner, B. Kirchner, H. Huber, *Chem. Phys.* **1997**, *224*, 253 – 261; b) P. M. Agrawal, B. M. Rice, D. L. Thompson, *J. Chem. Phys.* **2003**, *118*, 9680 – 9688; c) Y. Zhang, E. J. Maginn, *J. Chem. Phys.* **2012**, *136*, 144116.
[19] a) R. H. Swendsen, J. S. Wang, *Phys. Rev. Lett.* **1986**, *57*, 2607 – 2609; b) D. J. Earl, M. W. Deem, *Phys. Chem. Chem. Phys.* **2005**, *7*, 3910 – 3916.
[20] a) B. J. Siwick, J. R. Dwyer, R. E. Jordan, R. J. D. Miller, *Science* **2003**, *302*, 1382 – 1385; b) Q. S. Mei, K. Lu, *Prog. Mater. Sci.* **2007**, *52*, 1175 – 1262.
[21] V. V. Kechin, *Phys. Rev. B* **2001**, *65*, 052102.
[22] P. Van't Zelfde, M. H. Omar, H. G. M. LePair-Schroten, Z. Dokoupil, *Physica* **1968**, *38*, 241 – 251.
[23] a) E. Pahl, F. Calvo, L. Koči, P. Schwerdtfeger, *Angew. Chem.* **2008**, *120*, 8329 – 8333; *Angew. Chem. Int. Ed.* **2008**, *47*, 8207 – 8210; b) E. Pahl, F. Calvo, P. Schwerdtfeger, *Int. J. Quantum Chem.* **2009**, *109*, 1812 – 1819.
[24] K. Patkowski, K. Szalewicz, *J. Chem. Phys.* **2010**, *133*, 094304.
[25] P. Schwerdtfeger, B. Assadollahzadeh, A. Hermann, *Phys. Rev. B* **2010**, *82*, 205111.
[26] G. Orkoulas, *J. Chem. Phys.* **2010**, *133*, 111104.
[27] a) D. Errandonea, R. Boehler, S. Japel, M. Mezouar, L. R. Benedetti, *Phys. Rev. B* **2006**, *73*, 092106; b) Y. A. Freiman, A. F. Goncharov, S. M. Tretyak, A. Grechnev, J. S. Tse, D. Errandonea, H.-K. Mao, R. J. Hemley, *Phys. Rev. B* **2008**, *78*, 014301.
[28] F. Senn, J. Wiebke, O. Schumann, S. Gohr, P. Schwerdtfeger, E. Pahl, unpublished results.
[29] F. Calvo, E. Pahl, M. Wormit, P. Schwerdtfeger, *Angew. Chem.* **2013**, *125*, 7731 – 7734; *Angew. Chem. Int. Ed.* **2013**, *52*, 7583 – 7585.
[30] A. Hermann, P. Schwerdtfeger, *Phys. Rev. B* **2009**, *80*, 064106.
[31] A. M. Ferrenberg, R. H. Swendsen, *Phys. Rev. Lett.* **1989**, *63*, 1195 – 1198.

 © 2013 Wiley-VCH Verlag GmbH & Co. KGaA, Weinheim